Use of 4D-printing and shape memory alloys to fabricate customized metal jewels with functional properties

Adelaide Nespoli, Nicola Bennato, Enrico Bassani and Francesca Passaretti
National Research Council – Institute of Condensed Matter Chemistry and Technologies for Energy (CNR-ICMATE, Lecco Unit), Via G. Previati 1/e, Lecco, Italy

Abstract

Purpose – This paper aims to examine customized NiTi jewels with functional properties fabricated through four-dimensional (4D)-printing.

Design/methodology/approach – Two opened rings are fabricated through selective laser melting starting from 55.2Ni-Ti (wt.%) micrometric powder. After the additive process the two rings present the one-way shape memory effect (OWSME). A specific training is accomplished on one of the two printed rings to promote the two-way shape memory effect (TWSME). Both the samples, namely, the rings, respectively, presenting the OWSME and TWSME property, follow a series of post-processing routes to improve the surface finish. Furthermore, a thermal treatment at high temperature is used to create a thin colored oxide layer on the sample surface.

Findings – Results show that the change of shape owing to the OWSME and TWSME properties allows the customized 4D-printed rings to be adaptable to environmental changes such as load and temperature variations. This adaptability improves comfort and fit of the jewels.

Originality/value – To the best of the authors' knowledge, in this work, first cases of additively manufactured NiTi jewels are reported to propose innovative solutions in the design and processing industry of jewels.

Keywords Additive manufacturing, NiTi, Shape memory effect, Jewelry, 4D-printing

Paper type Technical paper

Introduction

Additive manufacturing, also known as three-dimensional (3D)-printing, describes a family of technologies that fabricate 3D objects from a computer-aided design (CAD) model, layer after layer, whatever material is used (metal, plastic, concrete, hybrid, etc.). These technologies are characterized by a high level of freedom of design and enable the production of particulars with really complex geometries and small details, using material only where it is needed thus reducing the quantity of waste. Four-dimensional-printing takes place when the printed object is able to respond to external stimuli, as an example by changing the shape through an energy input. The additional fourth dimension is therefore given by the time that the printed object requires to perform a macroscopic shape transformation. Selective laser melting is the most used additive technique in the field of metals (DebRoy *et al.*, 2018; Herzog *et al.*, 2016; Song *et al.*, 2015; Gokuldoss *et al.*, 2017; Yap *et al.*, 2015; Yadroitsev and Smurov, 2010). It is a powder bed additive manufacturing that uses a laser beam source to selectively melt micrometric metal powder. The main issue of selective laser melting is the definition and tuning of several process parameters to fabricate a defect-free part with proper mechanical performance. The laser power, the laser scan speed, the hatch distance and the layer thickness are the most significant process parameters that play a significant role in determine the mechanical properties of the printed parts (Nespoli *et al.*, 2021; Bang *et al.*, 2021; Jadhava *et al.*, 2019; Ma *et al.*, 2020; Li *et al.*, 2018).

Among metals, near-equiatomic NiTi alloys represent a class of smart materials (shape memory alloys) that exhibit a macroscopic shape change through a modification of temperature or load. This is related to two peculiar properties known as shape memory effect and pseudoelasticity. Both the properties refer to a phase transition of the first-order solid-to-solid thermoelastic kind. They are promoted by a specific thermal treatment at high temperature which is also used to fix the shape to the material. Shape memory effect and pseudoelasticity are largely exploited in many industrial applications because they enable a mechanical energy that is used, respectively, to produce motion such as in actuators or sensors and to mitigate vibrations like in dampers.

The shape memory and the pseudoelastic shape recoveries are because of the existence of two different crystalline phases in the material stable at two different temperature ranges: austenite, stable at high temperature, and martensite, stable at low temperature, respectively, with body centered cubic and monoclinic cell (Figure 1a). Therefore, in stress-free condition, a suitable thermal cycle enables a microscopic phase change (Figure 1b).

The shape memory property consists in a macroscopic shape change through a thermal cycle that is chosen to enable the transition between the two solid phases. Two kinds of shape

The current issue and full text archive of this journal is available on Emerald Insight at: **https://www.emerald.com/insight/1355-2546.htm**

Rapid Prototyping Journal
28/5 (2022) 805–813
 [ISSN 1355-2546]
[DOI 10.1108/RPJ-06-2021-0156]

Received 30 June 2021
Revised 30 August 2021
Accepted 15 October 2021

Figure 1 (a) Representation of the austenite body centered cubic and the martensite monoclinic cells. (b) Schematization of the stress-free microscopic phase change through a thermal cycle

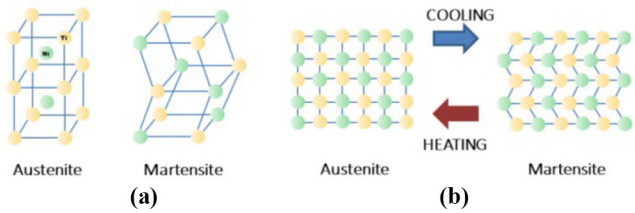

memory recovery can be promoted in NiTi. The one-way shape memory effect (OWSME) consists in the recovery of a pre-determinate austenite shape through heating a deformed martensite. Therefore, the application of an external load to martensite is essential to promote the OWSME. This property is reversible which means that the loaded austenite easily transforms in the deformed martensite through cooling (Figure 2a), and it is normally used to promote mechanical work. The OWSME material is prepared through a specific processing route that fixes the austenite shape by a single thermal treatment at high temperature (usually between 400 and 500°C) that is followed by a rapid cooling (normally water quench at room temperature, wq).

The second way to achieve a macroscopic shape change is the two-way shape memory effect (TWSME). It consists in the transformation between two different macroscopic geometrical shapes, each associated to one of the two solid phases, through a thermal loop. In this case, austenite transforms into the deformed martensite through cooling and without the help of an external load. The process is reversible, that is, the material transforms into austenite by increasing the temperature (Figure 2a). In the TWSME case, the material is prepared through a specific training that consists in a series of thermal cycles under an external load. There are various training methods (namely, repetitive routines) for obtaining TWSME, having the common feature of introducing irreversible defect in the structure (Nespoli *et al.*, 2014).

Pseudoelasticity is the ability of the material to transform from austenite to martensite through a change of load (stress-induced martensite) and at constant temperature. In this case, the transformation is isothermal and it occurs at austenite temperature. Because the stress-induced martensite is unstable at austenite temperature, the material freely recovers the austenite shape once the load is removed (Figure 2b). The pseudoelastic material is prepared through a thermal treatment at high temperature (in the 350–450°C range) followed by water quench at room temperature.

NiTi is the most industrially exploited shape memory alloy because of its high mechanical stability, high strain recovery, high damping property, biocompatibility and corrosion resistance thus finding numerous engineering applications. The main uses of NiTi are medicine (such as stents, grafts, orthopedic staples, orthodontic archwires, eyeglass frames, sutures; Petrini and Migliavacca, 2011; Wen *et al.*, 2018; Nespoli *et al.*, 2015), aerospace and military (such as couplers in F14 planes, morphing, low-shock release and deployment; Hartl and Lagoudas, 2007; Simiriotis *et al.*, 2021), safety (like damper and sprinklers; Huang *et al.*, 2020; Zhang *et al.*, 2020; Fang *et al.*, 2020; Huang *et al.*, 2020) and robotics (such as actuators; Copaci *et al.*, 2020; Nespoli *et al.*, 2010a, 2010b, 2012, 2014; Borlandelli *et al.*, 2015).

Besides, very few attempts in the use of shape memory alloys in jewelry have been presented. The most relevant are those reported in several patents. Huynh (2019) presented an article of jewelry based on the TWSME of shape memory alloys. In particular, the change of configuration is used to lock and unlock ornamental elements, thereby reducing the risk of loss of interchangeable ornamental elements. Ozawa *et al.* (1990),

Figure 2 (a) One-way and two-way shape memory effect; (b) pseudoelasticity

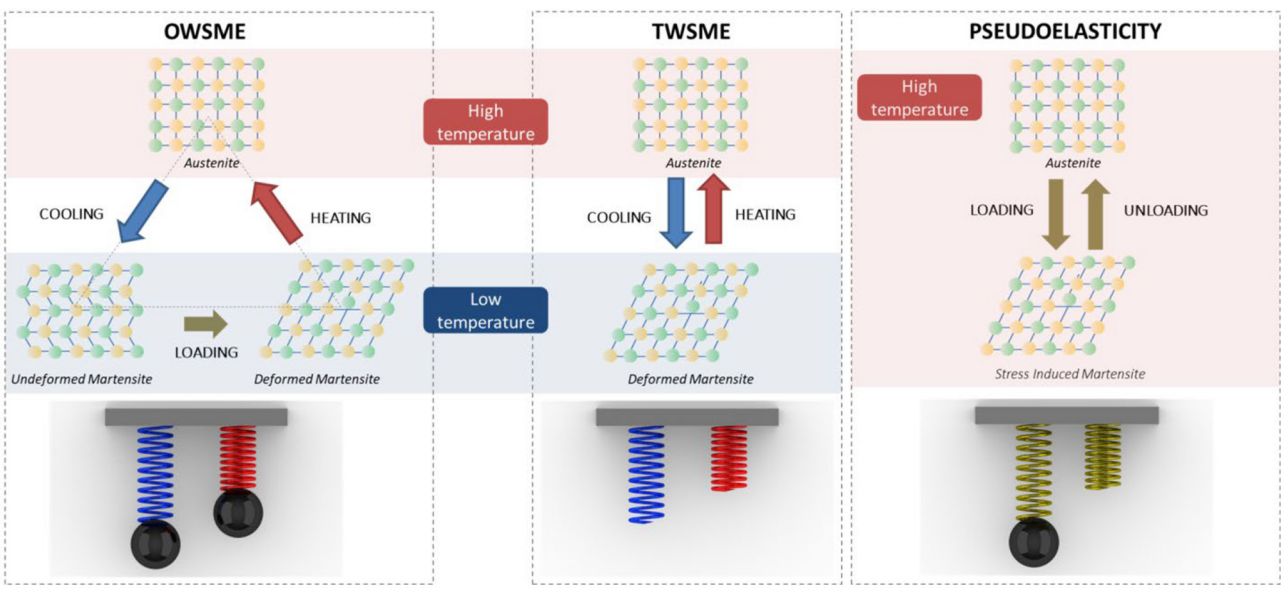

Mantovani and Galise (2012); and Wycisk *et al.* (1999) patented pseudoelastic ornaments based on NiTi wire core, support structures and cage-like elements. Herrera and Colas (2019) invented a jewelry item, such as a ring, which may vary in size through the shape memory property. Similarly, Hautcoeur (2008) and Beard (2005), respectively, presented jewels without claps and wire braid and bundles made of shape memory alloy elements. The shape memory property was also used by Holemans and Stalmans (2004a, 2004b) to change the gap between two end portions of a jewel. Holemans and Stalmans (2004a, 2004b) also presented shape memory alloy jewels that change the shape against a bias element that enables the restoring of the shape at low temperature.

Scientific literature presents very few works on this topic. Woff and Cortie (1994) reported on the use of the martensite transition to create a decorative spangling effect on AuCuAl based jewels, namely, Spangold. The change in the crystal structure in such alloys creates a unique surface finishing through the formation of many small facets on the previously polished surface. Besides, Besseghini *et al.* (2007) studied new gold alloys with shape memory alloy property, namely, AuCuZn and NiTiAu, mostly through thermal characterization.

Unfortunately, NiTi often presents a rather simple final geometry because of the poor machinability, low workability by plastic deformation and high work hardening. The difficult processing enables simple geometries such as wire, spring and tape (Nespoli *et al.*, 2010a, 2010b). This severely limits the use of NiTi, especially in the design and fashion industries such as jewelry where complex and innovative shapes are of great interest and often they are the primary objectives. The need of innovation in jewelry arises from the desire to have unique pieces that can be obtained through an intricate design. The recent spreading of metal additive manufacturing allowed to overcome the working limits of NiTi and permits the designers to look to new shapes potentially expanding the fields of application of NiTi.

The aforementioned works present jewelry items fabricated through conventional methods. The present work presents the first case studies of NiTi-based jewels fabricated through additive manufacturing. To this end, a selective laser melting machine is used to manufacture custom-made NiTi rings capable to adapt to environmental conditions (such as load and temperature). Thermal analysis is used to assess the phase transformation temperatures of the fabricated jewels. One-way and two-way shape memory properties are both explored through functional tests. Finally, polishing and oxide coloring are investigated to refine the final surface of the additively manufactured rings. Oxide coloring follows a thermal treatment that guarantees a Ni-free surface (Firstov *et al.*, 2001). Results are organized to highlight the functional performance and surface improvement of the fabricated parts.

Methods

The NiTi jewels were fabricated starting from a commercial near-equiatomic NiTi micrometric powder (TLS Technik GmbH & Co. Spezialpulver KG, Bitterfeld, Germany) containing about 55.2 wt.% of Ni. Figure 3 depicts a high-magnified image of the as-received NiTi powder taken through a scanning electron microscope (SEM LEO 1430). It can be noticed that the NiTi powder consists of spherical discrete particles with homogenous size approximately lower than 50 μm. Very few agglomerates are also discernable.

A Renishaw AM400 selective laser melting machine was used to fabricate the NiTi jewels. The process took place in inert atmosphere to reduce the risk of contamination with reactive gasses; to this end, before starting the process, the build chamber was filled with argon and oxygen content was kept at a value lower than 500 ppm. Furthermore, the jewels were fabricated on a NiTi platform in a reduced build volume ($78 \times 78 \times 54\ mm^3$).

The 3D CAD model of the jewels was obtained through Rhinoceros® software. The case studies consist in two rings, named *R*1 and *R*2. The STL file of the 3D models was elaborated by Magics® software which enabled a virtual representation of the build chamber and of the rings. In the virtual chamber, the rings were opportunely oriented to minimize the use of supports and to facilitate the removal from the build platform at the end of the process. A build processor of Renishaw was used to set the process parameters (Table 1) and to create the file readable from the AM400 machine. To enable near fully dense parts, the process parameters were selected within the ones studied by Nespoli *et al.* (2021).

A limited production of jewels is presented. In particular, three copies of *R*1 ring and four copies of *R*2 were produced. At the end of the process, each ring was removed from the build platform through a dremel. Subsequently, the ring surface was improved through mechanical polishing to remove the imperfections left by

Figure 3 Scanning electron microscope image of the as-received NiTi powder

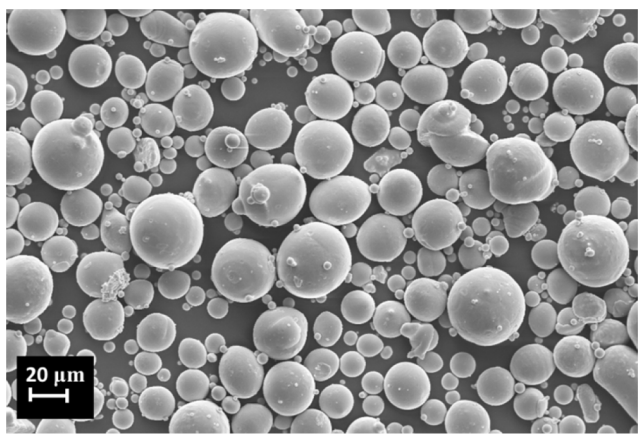

Source: Nespoli *et al.* (2021)

Table 1 Main process parameters of AM400 for the NiTi powder

Laser power [W]	250
Layer thickness [µm]	30
Hatch distance [µm]	100
Scan speed [mm/s]	1,000

Source: (Nespoli *et al.*, 2021)

the supports and through electro-polishing in a solution of 90% 2-butoxyethanol and 10% perchloric acid to enhance surface roughness. During electro-polishing, liquid nitrogen is used to hold the medium temperature at 0°C. The electrical tension between cathode (placed inside the medium) and anode (the sample) was set to 40 V. At the end of the electro-polishing process the sample was cleaned with alcohol and dried with hot air. The weight and the thickness of the sample were constantly monitored and the process ends at pre-determinate values. Mechanical refining through abrasive paste was finally accomplished to improve surface refinement.

The two as-built rings, *R*1 and *R*2, do not need a further thermal treatment to promote the shape recovery because both present the OWSME property with transformation temperatures that were assessed through differential scanning calorimetry (DSC25 TA Instruments) measurements. During thermal analysis, the sample followed a 10°C/min thermal cycle from 100 to −50°C; the phase transformation temperatures were detected through the tangent method.

TWSME training was accomplished on the *R*2 sample. The training consisted in ten thermal cycles. In each cycle, the *R*2 ring was first kept at martensite temperature for 4 min in a closed configuration. For this purpose, a homemade constrain was designed to tighten the two ends of the ring (Figure 4). Subsequently, the ring followed a free recovery at austenite temperature.

Finally, samples followed a thermal treatment at 600°C for 5 min in air (followed by quench in water) to promote thin colored and Ni-free oxide layer on the surface (Firstov *et al.*, 2001). A wild LED light stereo-microscope equipped with a polarizing filter was used to analyze the rings surface after the thermal treatment.

Table 2 summarizes the experimentations carried out on each ring copy.

Figure 4 Photograph of the constraint used in the TWSME training

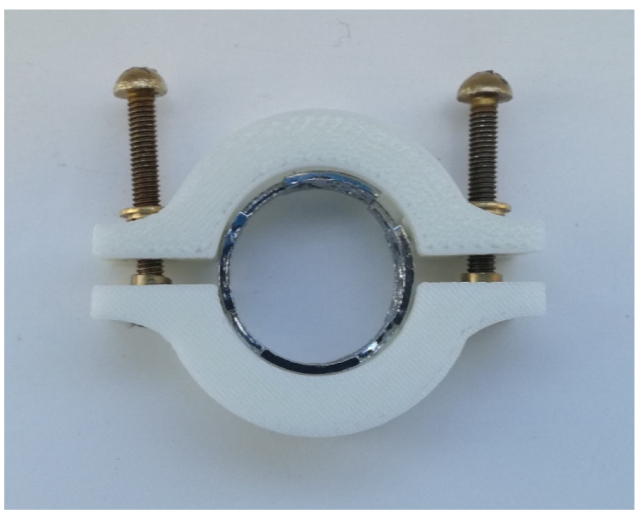

Results and discussion

Figure 5 reports the 3D CAD model of the two rings. Both of them have an aperture to facilitate the shape memory effect.

Figure 6 shows a photograph of the two rings at the end of the SLM process; it can be seen that the rings are fixed to the build platform through a ring-like support. This way of supporting was essential to avoid deformation of samples during the process resulting from internal stresses induced by the high heating-cooling

Figure 5 3D CAD model of *R*1 and *R*2 opened rings

Figure 6 *R*1 (a) and *R*2 (b) on the build platform at the end of the SLM process

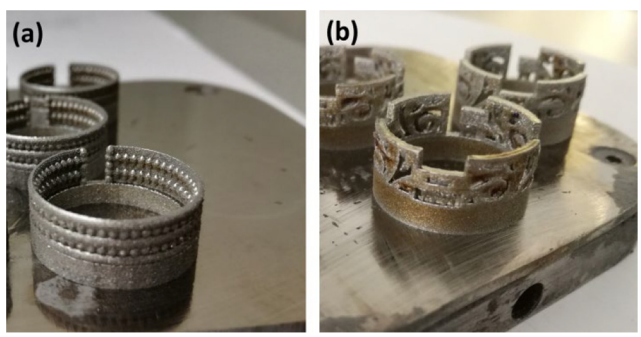

Table 2 Experimentations carried out on *R*1 and *R*2 rings

Specimen	Experimentation
1st copy of *R*1 and *R*2	Thermal analysis of as-built sample and study of the oxide coloring (rings were cut in 10–30 g pieces)
2nd copy of *R*1	Polishing + electro-polishing + OWSME functional test
2nd copy of *R*2	Polishing + electro-polishing + TWSME functional test
3rd copy of *R*1 and *R*2	Polishing + electro-polishing + mechanical refining with abrasive past + oxide coloring
4th copy of *R*2	Oxide coloring

rate typical of the SLM process. Figure 7 reports the two rings after the polishing routes.

Selective laser melting is a thermal process able to promote the shape memory effect in the NiTi as-built part. The transformation temperatures of the fabricated objects are reported in the DSC chart of Figure 8. In the graph, the characteristic temperatures are indicated as Ms, Mp and Mf for martensite start, peak and finish temperatures, respectively; As, Ap and Af for austenite start, peak finish temperatures. The transformation is completed in the (Mf, Af) range; however, it can be noticed that the (Mp, Ap) range well represents the year-round temperature variation. In this reduced temperature range the material can be easily transformed from partial austenite to partial martensite and vice versa through little variations of temperature.

Full and partial shape recovery was assessed through experimental observations. Figure 9 reports two photographs showing the OWSME functioning of the R1 ring. At room temperature the ring is deformed to have an aperture of approximately 2 mm. Upon heating up to a target temperature of 70°C, it recovers the austenite full opened shape (the one resulting from the SLM process); consequently, in this case a complete shape recovery is observed because the target heating temperature is higher than Af. However, the extent of shape recovery can be tuned with the temperature: the closer the target temperature is to Af and the higher degree of achieved aperture. This gives the ring a kind of self-accommodation to environmental temperature. Figure 10 reports 12 isolated freeze frames from a video shot during the shape recovery of *R*1 ring showing the partial recovery at different target temperatures.

Figure 11 shows two photographs of the ring trained to show the TWSME property, namely, the *R*2 sample. Magnifications of the apertures at the two characteristic phases are also reported. The martensite and austenite states are, respectively, achieved by immersing the ring in cold water and by placing the ring on a heating mat. In this case, the ring spontaneously change shape from martensite to austenite (and vice versa) by heating (and cooling)

Figure 7 *R*1 (a) and *R*2 (b) after the polishing routes

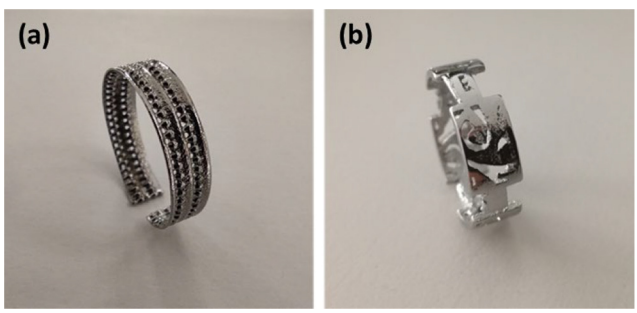

Figure 8 DSC graph of the as-built rings

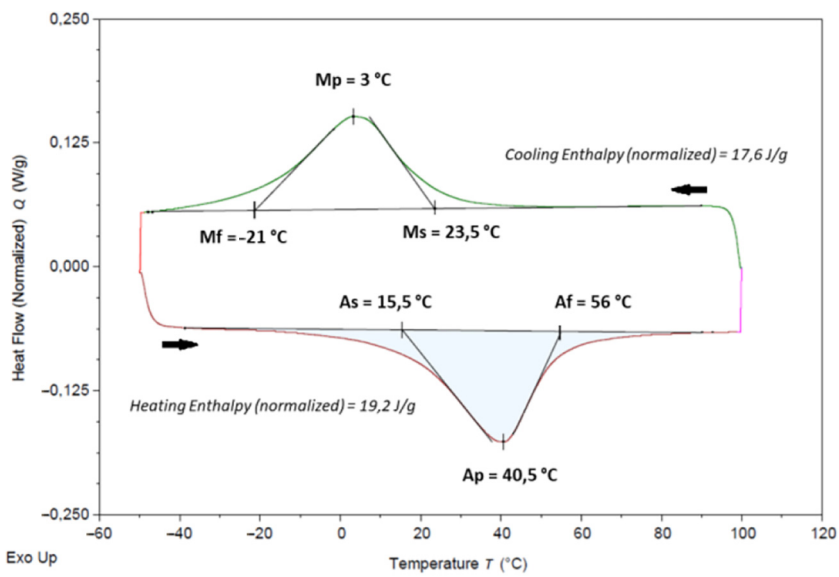

Note: Ms, Mp and Mf are the start, peak and finish martensite temperatures, respectively; As, Ap and Af are the start, peak and finish austenite temperatures, respectively

Figure 9 One-way shape memory effect of *R*1

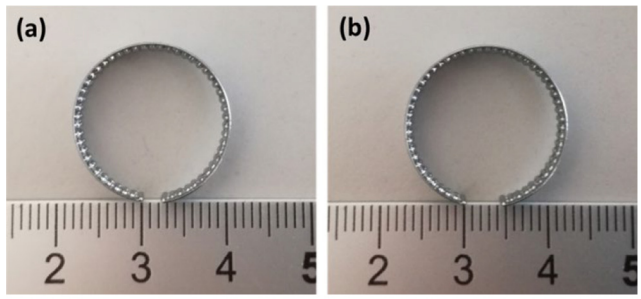

Notes: (a) Deformed martensite; (b) complete austenite shape recovery

Figure 10 Isolated frames of the shape recovery

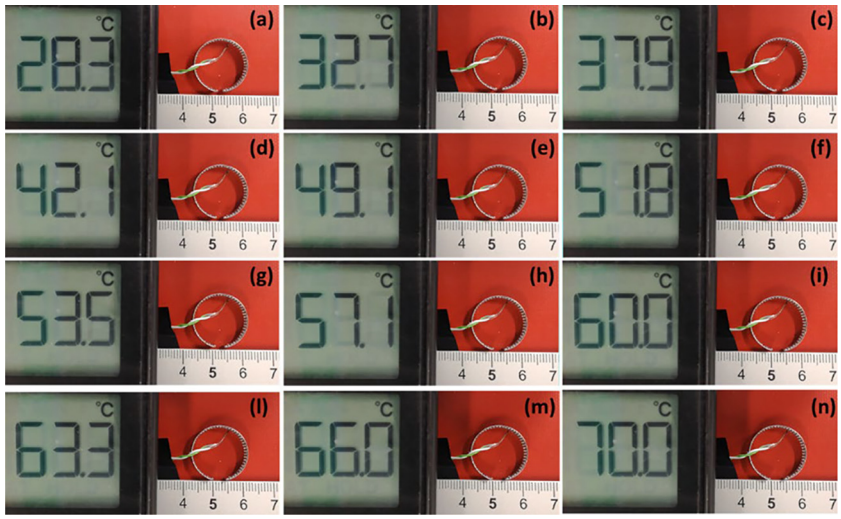

Figure 11 Two-way shape memory effect of *R*2 ring: martensite shape just after immersion in cold water and austenite shape after complete heating

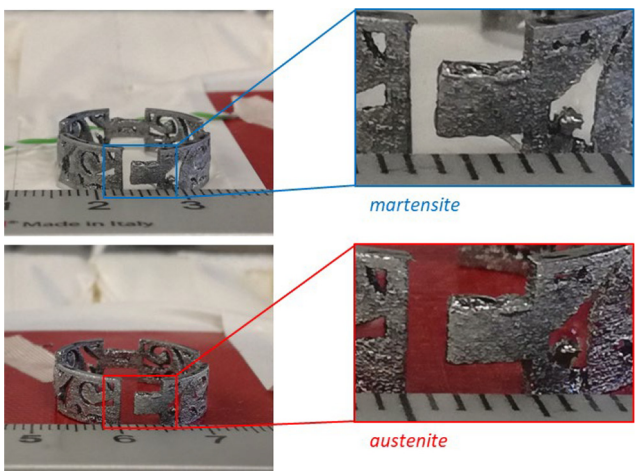

without external load. The degree of opening (and closure) is approximately 1 mm.

It is known that thermal treatment at temperatures of 600°C and above enables an oxide layer at the air/oxide interface of TiO_2 kind (Firstov *et al.*, 2001). In the present work, thermal oxidation is used to enhance the surface appearance of the printed jewels as well as to guarantee a Ni-free protective nickel-free oxide layer. It was observed that the weight and the surface finish of the fabricated rings affected the results of the oxide coloring obtained through the thermal treatment, see the photographs of Figure 12 and microscope observations of Figures 13–15. After polishing, *R*1 and *R*2 (that have different shape and weight) present two different colors despite having followed the same thermal treatment and polishing routes. In particular, *R*1 (0.514 g weight) has a predominately dark-grey colored surface with pink and dark purple sparse spots (Figures 12a and 13); polished *R*2 (1.334 g weight) shows a bright blue and purple surface with green and yellow regions (Figures 12b and 14). Similarly, comparing polished *R*2 and as-built *R*2 (1.422 g weight), respectively (Figure 12b,c), it can be highlighted that surface finish enables different coloring because the roughness surface of as-built *R*2 sample enables a predominantly green-yellow colored surface with diffused violet regions (see also Figure 15).

Figure 16 depicts the two sides of four samples of polished *R*2 ring (first copy) presenting different thermal treatment: as-built (S1), after annealing at 600°C for 5 min and water quenched (S2 and S3); after annealing at 600°C for 5 min and water quenched followed by a second annealing at 600°C for 3 min and water quenched (S4). It can be firstly noticed that S2 and S3 show a

Figure 12 Oxide coloring through the thermal treatment

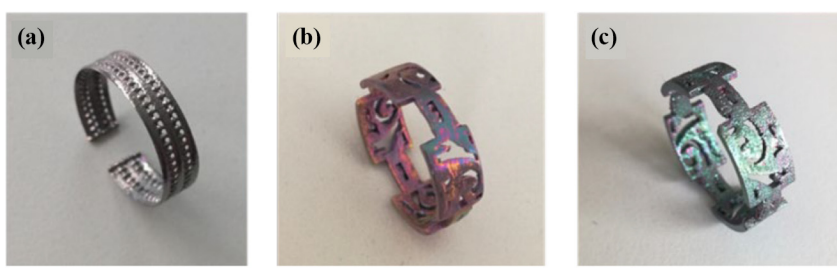

Notes: (a) Polished R1 ring; (b) polished R2 ring; (c) as-built R2 ring

Figure 13 Optical microscope observations of the polished *R*1 ring after the thermal treatment at 600°C for 5 min

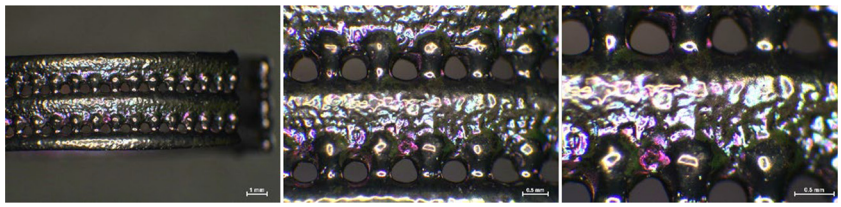

Figure 14 Optical microscope observations of the polished *R*2 ring after the thermal treatment at 600°C for 5 min

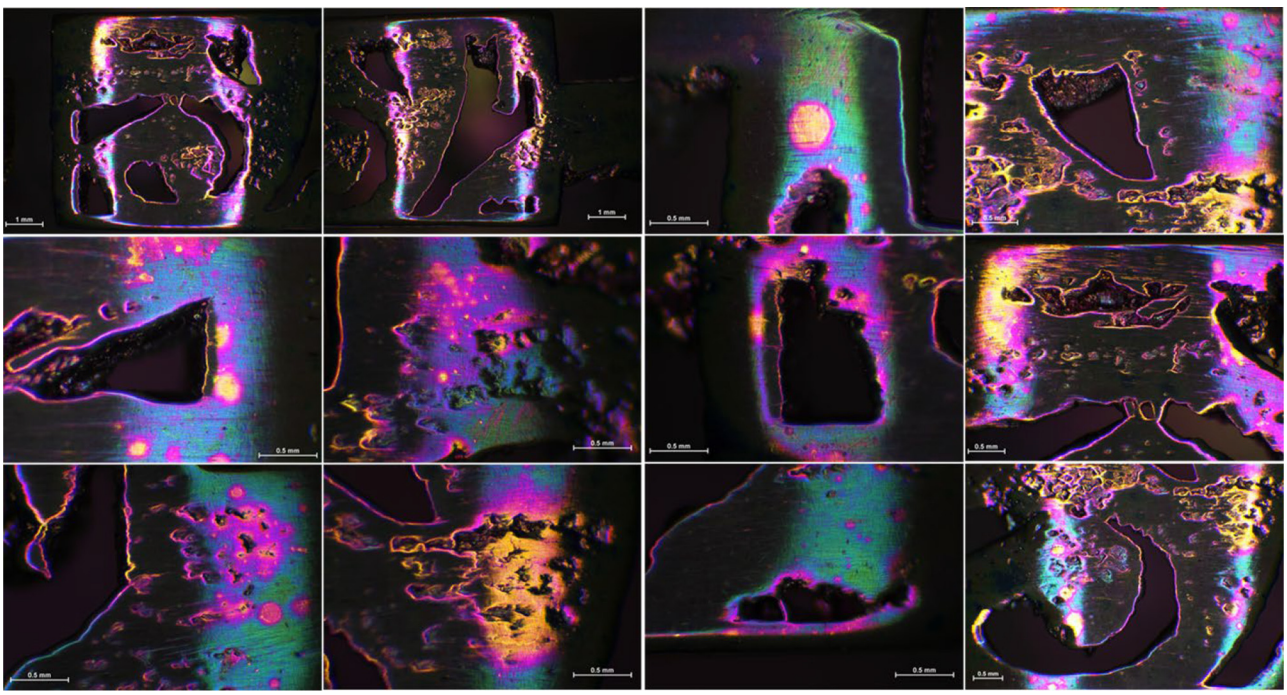

Figure 15 Optical microscope observations of the as-built *R*2 ring after the thermal treatment at 600°C for 5 min

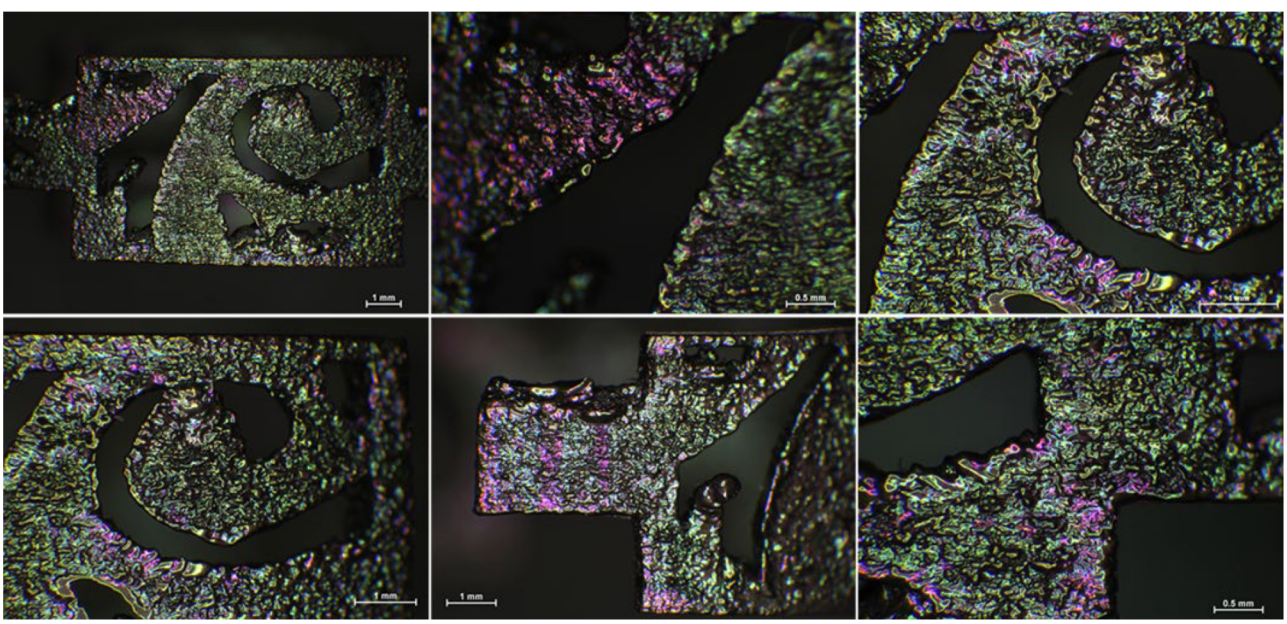

Figure 16 Two side of *R2* ring samples after thermal treatment

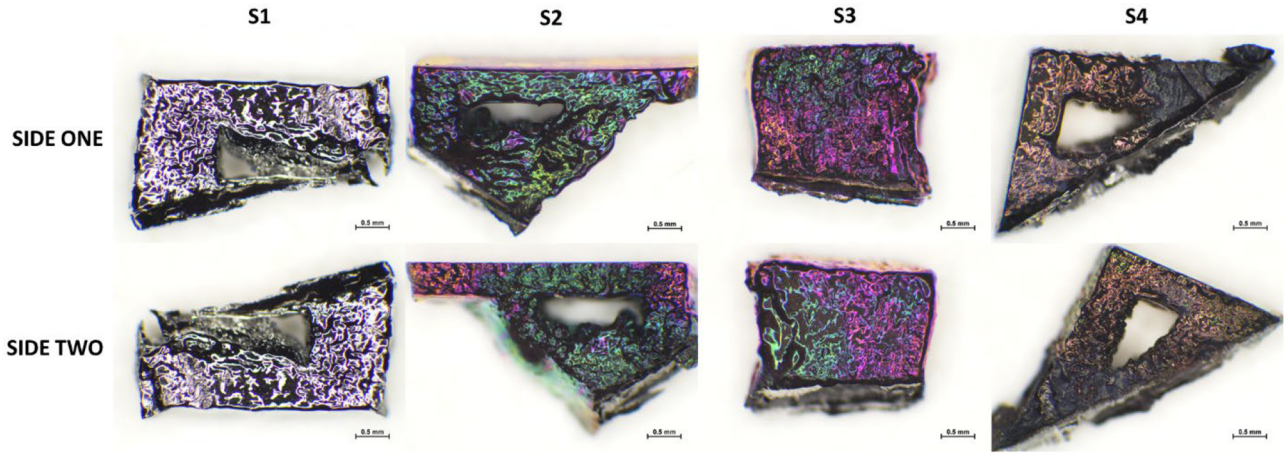

Notes: S1: as-built; S2 and S3: 600°C for 50; S4: 600°C 50 followed by 600°C for 30. Water quench was accomplished after each thermal treatment

similar surface coloring, confirming the one obtained on polished *R2* ring of Figure 14. *R2* ring surface appears brighter because of the final surface finish through abrasive paste. Furthermore, it can be observed that the surface color darkens with 600°C treatment time higher than 5 min.

Conclusions

In this work, first cases of additively manufactured NiTi jewels are studied to propose innovative solutions in the design and processing industry of jewels. A limited production of NiTi rings through selective laser melting is presented. This process enabled the fabrication of customized NiTi parts with unique shapes that could not be obtained through traditional technologies. Furthermore, the NiTi alloy provides functional property to the jewels such as the spontaneous recovery of a pre-defined shape by a change of temperature. This makes the ring particularly adaptable to environmental temperature thus ensuring a comfortable wearability and improved fit, such as in case of finger swelling. The shape recovery is explored and verified through the OWSME and the TWSME. Results can be summarized as follows:

- Case of OWSME: At austenite temperature the ring diameter is the one defined by the CAD model. At low temperature (that is in martensite state) the ring can be manually deformed to smaller size to adapt to thin fingers. With the increasing of temperature, the size of the ring increases because the material gradually recovers the austenite shape. The OWSME needs the ring to be deformed in the martensite state.
- Case of TWSME: The ring is trained to freely change the shape between two temperatures (the martensite and the austenite ones). At high temperature (austenite state) the size of the ring increases (to the CAD model ones). A decreasing of the size is observed upon cooling to martensite temperature (to the trained dimension). This happens autonomously because the ring has memorized the two shapes through the training route.

Moreover, the surface of the NiTi printed part can be further improved by thermal oxidation which gives the printed jewel both a peculiar coloring and a Ni-free surface making the proposed fabrication method and post processes attractive to the jewel design industry.

Finally, because of the experimental nature of the proposed work, the estimation of manufacturing time and costs of the proposed items is hazardous. However, the presented fabrication route can be easily transferred to more complex shapes.

References

Bang, G.B., Kima, W.R., Kim, H.K., Park, H.K., Kim, G.H., Hyun, S.K., Kwon, O. and Kim, H.G. (2021), "Effect of process parameters for selective laser melting with SUS316L on mechanical and microstructural properties with variation in chemical composition", *Materials & Design*, Vol. 197, p. 109221.

Beard, G. (2005), "Manufacturing method for jewelry including shape memory alloy elements", US 6910,73 B2.

Besseghini, S., Passaretti, F., Villa, E., Fabbro, P. and Ricciardi, F. (2007), "Gold with a martensitic transformation: which opportunities?", *Gold Bulletin*, Vol. 40 No. 4, pp. 328-335.

Borlandelli, E., Scarselli, D., Nespoli, A., Rigamonti, D., Bettini, P., Morandini, M., Villa, E., Sala, G. and Quadrio, M. (2015), "Design and experimental characterization of a NiTi-based, high-frequency, centripetal peristaltic actuator", *Smart Materials and Structures*, Vol. 24 No. 3, p. 35008.

Copaci, D.-S., Blanco, D. and Moreno, A. and M-C, L. (2020), "Flexible shape memory alloy actuators for soft robotics: modelling and control", *International Journal of Advanced Robotic Systems*, Vol. 17 No. 1, pp. 1-15.

DebRoy, T., Wei, H.L., Zuback, J.S., Mukherjee, T., Elmer, J. W., Milewski, J.O., Beese, A.M., Wilson-Heid, A., Ded, A. and Zhang, W. (2018), "Additive manufacturing of metallic components – process, structure and properties", *Progress in Materials Science*, Vol. 92, pp. 112-224.

Fang, C., Liang, D., Zheng, Y., Yam, M.C.H. and Sun, R. (2020), "Rocking bridge piers equipped with shape memory alloy (SMA) washer springs", *Engineering Structures*, Vol. 214, p. 110651.

Firstov, G.S., Vitchev, R.G., Kumar, H., Blanpain, B. and Van Humbeeck, J. (2001), "Surface oxidation of NiTi shape memory alloy", *Biomaterials*, Vol. 23 No. 24, pp. 4863-4871.

Gokuldoss, P.K., Kolla, S. and Eckert, J. (2017), "Additive manufacturing processes: selective laser melting, electron beam melting and binder jetting—selection guidelines", *Materials*, Vol. 10 No. 6, p. 672.

Hartl, D.J. and Lagoudas, D.C. (2007), "Aerospace applications of shape memory alloys", *Proceedings of the Institution of Mechanical Engineers, Part G: Journal of Aerospace Engineering*, Vol. 221 No. 4, pp. 535-552.

Hautcoeur, A. (2008), " "Bijou sans fermoir en alliage à mémoire de forme", FR2936686 A1 France

Herrera, B. and Colas, D. (2019), "Jewellery item", EP3572549 A1 European Patent Office

Herzog, D., Seyda, V., Wycisk, E. and Emmelmann, C. (2016), "Additive manufacturing of metals", *Acta Materialia*, Vol. 117, pp. 371-392.

Holemans, T. and Stalmans, R. (2004a), "Jewellry arrangements", US 204/0025984 A1

Holemans, T. and Stalmans, R. (2004b), "Shape memory device for changing shape at small temperature changes", US 2004/0221614 A1

Huang, H., Mosalam, K.M. and Chang, W.-S. (2020), "Adaptive tuned mass damper with shape memory alloy for seismic application", *Engineering Structures*, Vol. 223, p. 111171.

Huynh, C. (2019), "Jewelry that reversibly transitions between two different configurations", *WO 2019/070386 A2*

Jadhava, S.D., Dadbakhsh, S., Goossens, L., Kruth, J.P., Van Humbeeck, J. and Vanmeensel, K. (2019), "Influence of selective laser melting process parameters on texture evolution in pure copper", *Journal of Materials Processing Technology*, Vol. 270, pp. 47-58.

Li, Z., Kucukkoc, I., Zhang, D.Z. and Fei Liu, F. (2018), "Optimising the process parameters of selective laser melting for the fabrication of Ti6Al4V alloy", *Rapid Prototyping Journal*, Vol. 24 No. 1, pp. 150-159.

Ma, Z., Zhang, K., Ren, Z., Zhang, D.Z., Tao, G. and Xu, H. (2020), "Selective laser melting of CueCreZr copper alloy: parameter optimization, microstructure and mechanical properties", *Journal of Alloys and Compounds*, Vol. 828, pp. 154350.

Mantovani, G. and Galise, F. (2012), "Variable-shape piece of jewellery", WO2012/001713A1

Nespoli, A., Bassani, E., Besseghini, S. and Villa, E. (2010a), "Rotational mini-actuator activated by two antagonist shape memory alloy wires", *Physics Procedia*, Vol. 10, pp. 182-188.

Nespoli, A., Besseghini, S., Pittaccio, S., Villa, E. and Viscuso, S. (2010b), "The high potential of shape memory alloys in developing miniature mechanical devices: a review on shape memory alloy mini-actuators", *Sensors and Actuators A: Physical*, Vol. 158 No. 1, pp. 149-160.

Nespoli, A., Dallolio, V., Villa, E. and Passaretti, F. (2015), "A new design of a nitinol ring-like wire for suturing in deep surgical field", *Materials Science and Engineering: C*, Vol. 56, pp. 30-36.

Nespoli, A., Grande, A.M., Bennato, N., Rigamonti, D., Bettini, P., Villa, E., Sala, G. and Passaretti, F. (2021), "Towards an understanding of the functional properties of NiTi produced by powder bed fusion", *Progress in Additive Manufacturing*, Vol. 6 No. 2, pp. 321-337.

Nespoli, A., Rigamonti, D., Villa, E. and Passaretti, F. (2014), "Design, characterization and perspectives of shape memory alloy elements in miniature sensor proof of concept", *Sensors and Actuators A: Physical*, Vol. 218, pp. 142-153.

Nespoli, A., Villa, E. and Besseghini, S. (2012), "Thermo-mechanical properties of snake-like NiTi wires and their use in miniature devices", *Journal of Thermal Analysis and Calorimetry*, Vol. 109 No. 1, pp. 39-47.

Ozawa, K. Nakajima, E. and Yamagichu, I. (1990), "Ornament and method of manufacturing the same", US4943326

Petrini, L. and Migliavacca, F. (2011), "Biomedical applications of shape memory alloys", *Journal of Metallurgy*, Vol. 2011, pp. 1-15.

Simiriotis, N., Fragiadakis, M., Rouchon, J.F. and Braza, M. (2021), "Shape control and design of aeronautical configurations using shape memory alloy actuators", *Computers & Structures*, Vol. 244, p. 106434.

Song, B., Zhao, X., Li, S., Han, C., Wei, Q., Wen, S., Liu, J. and Shi, Y. (2015), "Differences in microstructure and properties between selective laser melting and traditional manufacturing for fabrication of metal parts: a review", *Frontiers of Mechanical Engineering*, Vol. 10 No. 2, pp. 111-125.

Wen, C., Yu, X., Zeng, W., Shan Zhao, S., Wang, L., Wan, G., Huang, S., Grover, H. and Chen, Z. (2018), "Mechanical behaviors and biomedical applications of shape memory materials: a review", *AIMS Materials Science*, Vol. 5 No. 4, pp. 559-590.

Woff, I.M. and Cortie, M.B. (1994), "The development of spangold", *Gold Bulletin*, Vol. 27 No. 2, pp. 44-54.

Wycisk, J. Ehrlinspiel, M. and Schuesler, A. (1999), "Jewellery article is made from material having shape memory effect and super-elastic behaviour thermally treated into final shape", DE19934312 A1 Germany,

Yadroitsev, I. and Smurov, I. (2010), "Selective laser melting technology: from the single laser melted track stability to 3D parts of complex shape", *Physics Procedia*, Vol. 5, pp. 551-560.

Yap, C.Y., Chua, C.K., Dong, Z.L., Liu, Z.H., Zhang, D.Q., Loh, L.E. and Sing, S.L. (2015), "Review of selective laser melting: materials and applications", *Applied Physics Reviews*, Vol. 2 No. 4, p. 41101.

Zhang, Z., Bi, K., Hao, H., Sheng, P., Feng, L. and Xiao, D. (2020), "Development of a novel deformation-amplified shape memory alloy-friction damper for mitigating seismic responses of RC frame buildings", *Engineering Structures*, Vol. 216, p. 110751.

Corresponding author

Adelaide Nespoli can be contacted at: adelaide.nespoli@cnr.it